Atmos. Chem. Phys. Discuss., 11, 31231–31263, 2011
www.atmos-chem-phys-discuss.net/11/31231/2011/
doi:10.5194/acpd-11-31231-2011

Atmospheric Chemistry and Physics Discussions

Dust resuspension under weak wind conditions: direct observations and model

O. G. Chkhetiani[1,2], E. B. Gledzer[1], M. S. Artamonova[1], and M. A. Iordanskii[3]

[1]A.M. Obukhov Institute of Atmospheric Physics, Russian Academy of Sciences, Moscow, Russia
[2]Space Research Institute, Russian Academy of Sciences, Moscow, Russia
[3]State institution "Karpov Physics and Chemistry Institute", Moscow, Russia

Received: 13 July 2011 – Accepted: 14 October 2011 – Published: 25 November 2011

Correspondence to: O. G. Chkhetiani (ochkheti@rssi.ru)

Published by Copernicus Publications on behalf of the European Geosciences Union.

Abstract

Here we report the results of the direct observations of fine scale mineral dust aerosol carried out over extensive sand areas in desertificated lands of Kalmykia in 2007, 2009 and 2010 under conditions of weak wind and strong heating of the surface with near absence of saltation processes. Measurements show that the fine mineral dust aerosol in the chosen region constitutes a considerable fraction of the entire air aerosol in the atmospheric surface layer (in terms of both the number of particles and their mass). Data of fine aerosol mass concentrations are treated on the basis of physical model estimates obtained for fluid dynamic parameters in the viscous thermal boundary layer near the ground surface. The deviations of mass concentrations from background are linked to temperature drop in the thermal layer near the surface and the value of friction velocity.

1 Introduction

A source of atmospheric mineral aerosols is the underlying surface, which emits particles into the atmosphere under certain conditions. The atmospheric dust is an important faction in shaping not only regional climates but also general climate (IPCC Fourth Assessment Report IPCC IV, 2007). The present models of dust resuspension are concentrated on the wind saltation as the main mechanism for dust resuspension. However, observations in deserts clearly show the presence of mineral dust in the atmosphere at no winds or weak winds (Golitsyn et al., 2003).

Experimental data and theoretical estimates show that particle detachment from the ground surface can be associated with turbulent stresses created by the velocity shear in the surface boundary layer. This mechanism occurs when the friction velocity u_* reaches a critical value of about $0.5\,\mathrm{m\,s^{-1}}$ (see Barenblatt and Golitsyn, 1974, and the references therein). The friction velocity $u_* = \langle -u'v' \rangle^{1/2}$ is proportional to turbulent velocity fluctuations and determines the thickness δ_* of the viscous boundary layer near the (smooth) underlying surface: $\delta_* \approx 5\frac{\nu}{u_*}$, where $\nu \approx 1.3 \times 10^{-5}\,\mathrm{m^2\,s^{-1}}$ is the kinematic viscosity of air (Monin and Yaglom, 1971); for flows above water surface and other types of underlying surfaces with various roughness, some expressions of the numerical coefficients in the formula for the viscous sublayer thickness can be found in Foken (1978, 2008). For the indicated values of u_*, the value of δ_* is on the order of 100 µm. When u_* reaches the critical values determined by the ground surface and relief properties, particles whose size is larger than δ_* can be, depending on their mass and the degree of surface cohesion, pulled away from the viscous sublayer. They are then lifted by turbulent velocity fluctuations and participate in the saltation processes as one of the sources of fine aerosol fraction.

A different situation occurs when size D of dust particles is much smaller than δ_* ($D \sim 0.1$–10 µm). Such particles are completely immersed in the viscous sublayer, where the turbulent wind stresses decrease sharply and cannot overcome the particle cohesion. The situation is further complicated by the fact that, in reality, particles of these sizes are situated in cavities or pores between roughness elements formed by large-size particles or form aggregate particles of various sizes. Nevertheless, experimental data suggest that even submicron dust particles are present in the atmosphere. There have been several mechanisms proposed to explain this phenomenon. The most popular ones are (i) the saltation mechanism (when particles with a size about 100 µm are pulled away from the surface and then fall back and knock out smaller particles) and (ii) the mechanism based on particle electrification (see Yablokov and Andronova, 1997). Mechanism (i) is directly associated with the effect exerted by fairly strong turbulent velocity fluctuations on average-size particles. This takes place only when the mean wind speed on the outer edge of the surface boundary layer exceeds a sufficiently large value of $\sim 10\,\mathrm{m\,s^{-1}}$. However, the number of atmospheric fine particles and the conditions for their occurrence suggest that they can also be lifted in calm weather, when the wind force is insufficient to form strong shear turbulence over the underlying surface. For example, according to estimated characteristics of fine dust particles lifted in the atmospheric surface boundary layer of Mars, the wind speed must be such that

u_* is higher than $4\,\mathrm{m\,s^{-1}}$, which is not observed, while local dust storms are frequent events (Greeley and Iversen, 1985) (see Golitsyn, 1980; the kinematic viscosity for the Martian atmosphere is on the order and larger than for Earth, so to get $\delta_* \approx 100\,\mu\mathrm{m}$ the values of u_* should be increased, see also Larsen et al., 2002).

Direct measurements of submicron aerosol concentrations (0.1–1.0 µm) in the desert conditions at a calm low wind weather when saltation processes are relaxed; though rare enough, there are data for this size in conditions of dust devil formation Gillette and Sinclair (1990); Gillette et al. (1993). There are also laboratory measuring of concentrations of dust fraction up to 10 µm at its resuspension for lack of a saltation (Loosmore and Hunt, 2000; Gillette et al., 2004).

Observed data of aerosol concentrations, including fine size particles, in desertificated lands of Kalmykia in 2007, 2009 and 2010 under conditions of a light breeze and strong heating of the soil (heat fluxes on a surface $f \sim 200$–$500\,\mathrm{W\,m^{-2}}$) are analyzed. It should be stressed that presented data were obtained in conditions of a near lack of saltation on a sand surface ($u_* < 0.5\,\mathrm{m\,s^{-1}}$). Concentrations near the surface (an aerosol source) at height 0.5 m are compared to values at levels of 2 or 1.5 m, which for the yielded requirements of calm weather can come close to the background values.

Temperature measurements show that the air above a sand layer is in convective motion due to the heating of the layer up to temperatures of ∼ 40–70 °C (Golitsyn et al., 2003). In an air layer ∼ 0.5–1 m thick, the above temperature falls sharply (about 10–30 K). Moreover, most of this temperature fall occurs within the first centimeter from the sand surface. In the same manner as for pure shear turbulence with a viscous boundary layer of thickness δ_* and with the characteristic fluctuation velocity u_*, the lift of sand and aerosol by convective turbulence is determined by the thickness δ_T of the convective boundary layer (in which the above temperature falls sharply) and by the characteristic convective horizontal velocity u_T at the outer boundary-layer edge. Aerosol resuspension expressed in mass units (e.g., the aerosol mass concentration ΔC, which is the difference between the mass concentrations at two levels – near the surface and above the thermal boundary layer) is found to be proportional to the velocity amplitude u_T: $\Delta C \sim u_\mathrm{T}$. The actual proportionality constant depends on the properties of the aerosol, soil, and relief. A more accurate dependence would be $\Delta C \sim u_\mathrm{T} - u_{T_\mathrm{cr}}$ for $u_\mathrm{T} > u_{T_\mathrm{cr}}$, where u_{T_cr} is the critical convective velocity, below which there is no aerosol resuspension. For strongly heated soil, u_T is higher than the critical value. For controlled shear flows with large values of u_*, there are several sand flux formulas, beginning with Bagnold's $\sim u_*^3$ (Bagnold, 1941), which depends on the friction velocity. Some of the approximations with the friction velocity threshold $u_{*\mathrm{cr}}$ $u_{*\mathrm{cr}}$ are described in Zhou et al. (2002); Kok and Renno (2009) (see also Shao, 2000).

2 Field measurements

2.1 Measurements and external parameters

The aerosol resuspension from the soil under conditions of calm weather have been investigated during Kalmykian expeditions in July 2007, 2009, and 2010. The republic Kalmykia is located in the southeastern part of European Russia. In general, this region represents semi-desertic territory with the extensive sandy areas covered with ridges of dunes. Also, there are large, dried and half-dried salt lakes.

The observations were made in two places. The first place with the coordinates 45°17′06″ N 45°53′12″ E (2007, 2009) lies a distance of 20 km southwest of the Komsomolsky village. The second place with the coordinates 45°25′52″ N 46° 26′28″ E (2010) lies a distance of 30 km east of the Komsomolsky village. The sand areas observed in 2007 and 2009 measure 700 m × 200 m and the one observed in 2010 measures 1600 m × 600 m. These areas extend from northwest to southeast. Rare dunes of heights less than 1.5 m were outside the measurement area. This choice of a duneless area was made to reduce the fetch effects, so that fine aerosol was emitted directly from the soil due to thermal or weak wind action rather than by blowing off the tops of dunes and other ground elevations. Probably, the fetch effects on observations cannot be completely eliminated, especially in strong wind gusts. The structure of the atmospheric boundary layer and processes related to arid aerosol emission were measured simultaneously.

The aerosol concentration was measured during the daytime (usually from 09:00 to 19:00) at two levels (0.5 and 2.0 m in 2007 and 2010; 0.5 and 1.5 m (in 2009)) with laser aerosol counters (LAC) (8 channels 0.15–1.5 µm) and a Royco aerosol counter (9 channels 0.5–15 µm). Air samples for determining the aerosol composition were taken separately.

The daytime wind speed, air temperature, and humidity at levels 0.2, 0.5, 1.0, 2.0, 3.0, and 5.0 m were continuously measured. Additionally, the temperature and humidity of the surface were measured with five sensors placed around the base of the aerosol counters at approximately 1–2 m. The ground surface sensors were covered with a very thin sand layer to reduce the direct radiation effects. In clear sky weather, the surface temperature of the sand was 60–70 °C. Simultaneously, the air temperature at a level of 3 m was about 40 °C and the wind speed at 2 m ranged from 1.7 m s^{-1} to 5.5 m s^{-1}. The daytime heat fluxes varied from 200 to 350 W m^{-2} with spikes up to 500 W m^{-2}.

The friction velocity was calculated according to the Monin–Oboukhov theory from the speed differences at different levels (0.5 and 2 m) and was 0.05–0.5 m s^{-1}. For data representation we have used the more simple variant u_*. We calculated u_* from the measured mean horizontal velocity $u(z)$ at the height $z = 3$ m by using the formula $u_* = \kappa u(z)/\ln(z/z_0)$, where $z_0 = 10^{-4}$ m and $\kappa = 0.4$ is the von Karman constant. This simple formula presented above produces satisfactory estimates of the turbulent fluctuation intensity in the boundary layer and does not require additional assumptions.

For the data discussed below (for example, 28 and 29 July 2007), the characteristic vertical velocity w_T in the viscous thermal boundary layer (see below Eq. 7) ranges from 0.007 to 0.015 m s^{-1}. The Stokes settling velocity is determined as (Shao, 2000)

ACPD
11, 31231–31263, 2011

$$w_t(d) = \left(\frac{4\rho_p g d}{3\rho C_d(Re_t)}\right)^{1/2},$$

$$C_d(Re_t) = \frac{24}{Re_t}(1 + 0.15 Re_t^{0.687}), \quad (1)$$

where $Re_t = w_t d/\nu$, ρ_p is the dust density, ρ is the air density, g is the gravity acceleration, d is the size of particles. The size of dust particles with a density 2.6×10^3 kg m^{-3} having the settling velocity the same order with the specified above values (0.007–0.015 m s^{-1}) would be 10–15 µm in diameter. Thus, a fine aerosol detached and lifted from the surface is easily carried away into the atmosphere.

2.2 The sizes and mass distributions

Distributions of aerosol particles in 2007 (Figs. 1a and 2a) and in 2009 (Figs. 1b and 2b) are shown. Figure 1a,b represents the daytime-averaged at 2 m (2007) and 1.5 m (2009) distributions of aerosol particles, which depend on the sizes of particles. Figure 2a,b represents aerosol mass concentrations, depending on the sizes of particles. The mass distributions $\Delta M/\Delta \log(d)$ were calculated according to the technique of Junge (1963), which roughly corresponds, up to constants, to the function $d^3 \Delta N/\Delta \log(d)$. It is well seen that the basic aerosol mass is concentrated on small scales on days with moderate wind, while large-size particles appear at stronger winds: $V(2) > 4.8$ m s^{-1} ($V(2)$ – daytime-averaged horizontal velocity at 2 m) for measurements in 2007 and $V(2.2) > 4.0$ m s^{-1} for measurements in 2009. Figure 1a,b shows that the fraction of submicron particles considerably exceeds in number the fraction of particles with sizes more than 1 µm. Even in terms of mass (Fig. 2a,b), the fraction of 0.1–0.6-µm particles is comparable to that of 0.6–8-µm particles. The 23–25 July 2007 distributions stand out due to their large submicron aerosol fractions. However, this is due to the overcast rainy conditions occurring on 23 and 24 July 2007. In fact, steady

ACPD
11, 31231–31263, 2011

observation conditions were from 28 to 31 July 2007. The same conditions were for 23–27 July 2009 and 19, 27 July 2010 (with weak winds in the morning and moderate winds in the afternoon).

The convection in the near soil air boundary layer, as it follows from the estimates presented below, is defined by the temperature differences in the layer: for example, the difference δT between the ground surface temperature T_s and temperature at 0.2 m – $T_{0.2}$. In Fig. 3, the temperature differences $\delta T = T_s - T_{0.2}$ are shown as the dependence of T_s for the conditions with relative light wind. We see practically linear dependence for all surface temperature values. Also, for surface temperature T_s less than 31–33 °C, the differences δT on average are practically zero. This means that when the ground temperature is not widely different from the temperature of the ambient air, turbulent mixing near the surface smoothes the vertical temperature variations in near surface layer.

2.3 Mass concentrations and temperature differences

2.3.1 Small and moderate friction velocities

In Fig. 4, the deviations of the aerosol mass concentration values (µg m^{-3}) at 0.5 m ($C(0.5)$) from the 2-m ($C(2.0)$) (measurements 28/29 July 2007) and 1.5-m ($C(1.5)$) (measurements 24/26 July 2009, both in the morning) for particles 0.15–0.5 µm in size (2007) and 0.15–1.0 µm (2009), as a function of the temperature difference δT between the ground surface and 0.2 m, are presented for conditions of relative light wind (Fig. 4a,b for 2007, Fig. 4c,d for 2009). The winds shown in the insets of Fig. 1 are the average velocities at 2 m (2007) and 2.2 m (2009). The circles in Fig. 4 depict the values of ΔC, δT derived from concentrations measured for 1 min (the time required for the intake of air with aerosol in LAC and Royco counters).

The mass concentration was recalculated from the LAC-measured particle concentrations using the mean particle size for a given channel. For a given value of δT, a scatter in points corresponds to different values of u_*. However, if the variance of u_*

ACPD
11, 31231–31263, 2011

for different fixed δT is identical, then the width of the scatter area is also nearly identical for different δT. In Figs. 4, 6, and 7 the smooth line corresponds to the approximation of the data by power law $\Delta C \sim (\delta T)^{\alpha}$. For moderate values of u_* ($u_* < 0.3\,\mathrm{m\,s^{-1}}$), Fig. 4 suggests that the exponent α is $\alpha \approx 0.58$ (Fig. 4a), $\alpha \approx 0.52$ (Fig. 4b), $\alpha \approx 0.33$ (Fig. 4c), and $\alpha \approx 0.24$ (Fig. 4c).

The concentrations $C(2.0)$, $C(1.5)$ are regarded conditionally as the "background" values. As was noted above, the measurement conditions were chosen so that the influence of aerosol resuspension from the dunes surrounding the measurement area was minimal. However, even in this case, the concentrations $C(2.0)$, $C(1.5)$ cannot be regarded as absolute background values since they vary from day to day and depend on the humidity, temperature, and wind over a period of time preceding the measurements.

Apparent from the figures, values of differences ΔC for days of measuring in 2009 several times exceed quantities for 2007, reflecting various weather conditions for these years, in particular, more light breezes in 2009 that promoted aerosol accumulation in an air layer adjoining to soil surface.

Therefore, $C(2.0)$, $C(1.5)$ can be formally viewed as a background concentrations for several hours of daytime measurements. This is demonstrated in Fig. 5, which displays the mass concentrations $C(0.5)$, $C(2.0)$ (or $C(1.5)$) for particles 0.15–0.5 µm (0.15–1.0 µm) as a function of the temperature differences δT between the ground surface and 0.2 m for data of 29 and 30 July 2007 (a,b) and 23 and 24 July 2009 (c,d) with different wind conditions: for (a) $V(2) \approx 2.4\,\mathrm{m\,s^{-1}}$, for (b) $V(2) \approx 5.7\,\mathrm{m\,s^{-1}}$, for (c) $V(2.2) \approx 2.0\,\mathrm{m\,s^{-1}}$ (morning), for (d) $V(2.2) \approx 2.8\,\mathrm{m\,s^{-1}}$ (afternoon). Inspection of Fig. 5 shows that the values of $C(2.0)$ (for 2007) lie approximately in the range of 1.5–2 $\mathrm{\mu g\,m^{-3}}$, and $C(1.5)$ for 2009 in the range 3 $\mathrm{\mu g\,m^{-3}}$ (for 23 July) and 5 $\mathrm{\mu g\,m^{-3}}$ (for 24 July). Moreover, the values of $C(0.5)$ vary fairly strongly with the strength of wind (Fig. 5d).

ACPD
11, 31231–31263, 2011

2.3.2 Large friction velocities

For relative strong winds, the deviations ΔC of mass concentrations are shown in Fig. 6a (for 30 and 31 July 2007) and Fig. 6b (for 26 July 2009). For these days with sufficiently large u_* ($u_* \approx 0.3$-$0.4\,\mathrm{m\,s^{-1}}$), the exponent α is negative ($\alpha \approx -0.50$ in Fig. 6a, data of 30 July 2007; $\alpha \approx -0.35$ in Fig. 6a, data of 31 July 2007; $\alpha \approx -0.35$ in Fig. 6b, data of 26 July 2009). For such values of u_*, as δT increases, the aerosol mass concentration decreases as compared to the 2-m or 1.5-m values. The noted dependence on the friction velocity u_* (or the wind speed $u(z)$) is manifested in a twofold manner. On the one hand, it occurs via a decrease in the exponents α in the power law dependence. On the other hand, for the same difference δT (for example, $\delta T = 10\,\mathrm{K}$), as u_* rises (from Fig. 4a to Fig. 6a or Fig. 5a to 5b), ΔC increases 2–4 times. Thus, the possible approximation $\Delta C = \Delta C(u_*, \delta T)$ would give strong dependence on u_*. Unfortunately, empirical data are too scarce to construct such functions.

The difference between the morning and afternoon wind conditions can significally change the variance of deviations ΔC with temperature δT increasing. This is illustrated in Fig. 7a,b for the same day of 27 July 2009. The drop of ΔC was observed also for 23 July 2009 (afternoon). The results for 27 and 19 July 2010 are in Fig. 7c,d for weak and moderate values of wind.

Note that the scale of δT in Figs. 4–6 decreases with increasing u_* (from Figs. 4a to 6a or Fig. 5a to 5b). Obviously, this tendency reflects the fact that a heated surface is cooled to a greater degree when the wind above it is stronger (turbulent mixture in the layer). This is illustrated in Fig. 8 for small and moderate values of u_*.

Below, the field measured dependencies are discussed on the basis of the estimates of the main terms in the Boussinesq–Oberbeck equations, which describe the convection in viscous thermal boundary layer near the heated soil surface.

ACPD
11, 31231–31263, 2011

3 Motion in a convective viscous surface layer

Consider the motion of air near the boundary $z = 0$ of a heated soil layer. The convective layer under study is on the order of 1 cm thick. The temperature within it falls by ~ 10–$30\,^\circ$C from about 40–70 °C on the sand surface. Several formulas describing developed free convection in a layer heated from below can be found in Golitsyn (1980). They are developments of Oboukhov's (1946) and Monin–Oboukhov's (1954) theories presented in Obukhov (1971) and Lumley and Panofsky (1964) (for more full and recent references see Foken, 2008), and give expressions for the thickness δ_T of the boundary layer, in which the temperature decreases by δT (see Golitsyn, 1980):

$$\delta_\mathrm{T} \approx \frac{l_\nu}{2\beta_1 Pr^{1/3}} \left(\frac{T_0}{\delta T}\right)^{1/3}, \tag{2}$$

where $l_\nu = (\nu^2/g)^{1/3}$, $Pr = \nu/\kappa_\mathrm{T}$.

Above, ν is the kinematic viscosity. κ_T is the thermal diffusivity. T_0 is the surface temperature. The numerical coefficient $\beta_1 \sim 0.1$–0.2 can be found in Golitsyn (1980) (note that $1/2\beta_1$ is roughly equal to the numerical coefficient 5 in the approximate expression for the viscous boundary layer thickness δ_* in shear turbulence). The length scale l_ν in Eq. (2), which is determined by the viscosity and the acceleration due to gravity, is approximately equal to 3×10^{-4} m.

Formula (2) can easily be derived by estimating the basic terms in the Boussinesq–Oberbeck equations, assuming that the velocity of motion is low (viscous thermal boundary layer). Here, the temperature drop δT across the thermal boundary layer of thickness δ_T is assumed to be known. Below we use two assumptions of Gledzer et al. (2010). The first is that the viscous equations with low Reynolds numbers can be used within an approximately 1-cm thick layer overlying a heated ground surface. The vertical length scale is then much less than the horizontal one. The second assumption is that velocity variations in this layer are determined by two independent factors: namely, by thermal convection in the layer and by fluctuations due to the velocity shear

ACPD
11, 31231–31263, 2011

in the outer (turbulent) region above the viscous layer, which affect the velocity field in the thermal boundary layer via the upper boundary condition at $z = \delta_T$. From this, there appear two prescribed parameters δT and u_*, which determine the flow in the layer and the layer thickness. Next, the equations are used to estimate the basic parameters of convective flows in the viscous thermal boundary layer. The main goal of these estimates is to show that the empirical dependencies in Sect. 2 do not contradict the fluid dynamic equations for thermally stratified flows. This especially concerns the fact that the exponents in the power law dependence on ΔC reverse their sign with increasing u_*.

3.1 Basic equations and sublayers near the soil surface

Let w_T be the vertical velocity at the thermal boundary layer height $z \approx \delta_T$ and δT be the difference between the temperatures at the underlying surface ($z = 0$) and the boundary layer height δ_T. Estimating the orders of the quantities in the temperature deviation T' from T_0 equation of the Boussinesq–Oberbeck equations,

$$\frac{\partial T'}{\partial t} + (\boldsymbol{v}\nabla)T' = \kappa_T \Delta T' , \quad (3)$$

$$\frac{\partial w}{\partial t} + (\boldsymbol{v}\nabla)w = \nu\Delta w + g\frac{T'}{T_0} - \frac{1}{\rho_0}\frac{\partial p'}{\partial z} , \quad (4)$$

we have

$$\frac{w_T \delta T}{\delta_T} \sim \kappa_T \frac{\delta T}{\delta_T^2} , \quad (5)$$

$$\nu \frac{w_T}{\delta_T^2} \sim g\frac{\delta T}{T_0} , \quad (6)$$

Discussion Paper | Discussion Paper | Discussion Paper | Discussion Paper |
ACPD
11, 31231–31263, 2011
Dust resuspension under weak wind conditions
O. G. Chkhetiani et al.

which yields an estimate for w_T in terms of δ_T and horizontal velocity u_T for disturbances with length scale l:

$$w_T \sim \frac{\kappa_T}{\delta_T}\,, \tag{7}$$

$$\frac{u_T}{l} \approx \frac{w_T}{\delta_T}\,. \tag{8}$$

Combining Eqs. (5–8) gives Eq. (2) (without the numerical coefficient). Since the motion in a thin convective layer is quasi-horizontal, we assume that $l > \delta_T$.

Now, formulas (8) are extended to mean horizontal flows with vertical shear, which leads to the appearance of turbulent fluctuations proportional to u_*. Recall that velocity fluctuations with such an amplitude take place above the viscous sublayer, whose thickness δ_* is proportional to ν/u_*. In the viscous sublayer, taking into account that the wall is approached, the vertical and horizontal velocities fluctuations are estimated as linear functions for $z < \delta_*$

$$w(z) \approx u_* \frac{z}{\delta_*}\,, \tag{9}$$

$$u(z) \approx u_* \frac{z}{\delta_*} \tag{10}$$

and for $z > \delta_*$

$$w(z) \approx u_*\,, \tag{11}$$

$$u(z) \approx u_* \frac{z}{\delta_*}\,. \tag{12}$$

ACPD
11, 31231–31263, 2011

Dust resuspension under weak wind conditions

O. G. Chkhetiani et al.

3.2 The thermal velocity for low and high friction velocities

Assume that the vertical velocity w_T and horizontal velocity $u_\mathrm{T} \equiv u|_{z=\delta_\mathrm{T}}$ at $z = \delta_\mathrm{T}$ can be evaluated as the sum of the velocities due to a shear flow without convection (Eqs. 9–12) and estimates (Eqs. 7 and 8) for free convection. If the thickness δ_* of the viscous sublayer is larger than the thickness δ_T of the thermal layer $\delta_\mathrm{T} < \delta_*$ (i.e., u_* is still sufficiently low), then

$$w_\mathrm{T} \sim \frac{\kappa_\mathrm{T}}{\delta_\mathrm{T}} + u_* \frac{\delta_\mathrm{T}}{\delta_*}, \tag{13}$$

$$u_\mathrm{T} \sim w_\mathrm{T} \frac{l}{\delta_\mathrm{T}} + u_* \frac{\delta_\mathrm{T}}{\delta_*}, \tag{14}$$

where the first terms in the right-hand side (Eqs. 13 and 14) are caused by the thermal factors, and the second terms by the friction velocity due to the shear in the mean horizontal velocity.

For a high friction velocity u_*, when $\delta_\mathrm{T} > \delta_*$, we have

$$w_\mathrm{T} \sim \frac{\kappa_\mathrm{T}}{\delta_\mathrm{T}} + u_*, \tag{15}$$

$$u_\mathrm{T} \sim w_\mathrm{T} \frac{l}{\delta_\mathrm{T}} + u_* \frac{\delta_\mathrm{T}}{\delta_*}. \tag{16}$$

Using Eqs. (5) and (6) and expressions (Eqs. 13–16) for w_T, we obtain for δ_T and u_T

$$\delta_\mathrm{T} \sim d(q) \left(\frac{\nu^2}{g}\right)^{1/3} Pr^{-1/3} \left(\frac{\delta T}{T_0}\right)^{-1/3},$$

$$u_\mathrm{T} \sim gl \left(\frac{\kappa_\mathrm{T}}{g\nu^2}\right)^{1/3} \left(\frac{\delta T}{T_0}\right)^{2/3} d(q) \left(1 + \frac{u_*^2}{gl}\left(\frac{\delta T}{T_0}\right)^{-1}\right), \tag{17}$$

ACPD
11, 31231–31263, 2011

Dust resuspension under weak wind conditions

O. G. Chkhetiani et al.

where q is the dimensionless friction velocity

$$q = \frac{u_*}{(g\nu)^{1/3}} Pr^{1/6} \left(\frac{\delta T}{T_0}\right)^{-1/3}, \quad Pr = \frac{\nu}{\kappa_T}.$$

For d and q we have the equations (see details in Gledzer et al., 2010):

$$\begin{aligned} &d^3 - q^2 d^2 - 1 = 0, \quad qd < Pr^{1/2}, \\ &d^3 - Pr^{1/2} qd - 1 = 0, \quad qd > Pr^{1/2} \end{aligned} \tag{18}$$

The investigation of these equations gives the following asymptotic for u_T: for $u_* \sim u_1 = (g\nu)^{1/3}(\delta T/T_0)^{1/3} \sim 0.02$–$0.05\,\mathrm{m\,s^{-1}}$

$$u_T = \left(\frac{\delta T}{T_0}\right)^{2/3} C_1(l, \nu, \kappa_T), \quad C_1 \approx gl Pr^{-1/3}(g\nu)^{-1/3}; \tag{19}$$

for moderate values of $u_* \sim u_2 = (gl)^{1/2}(\delta T/T_0)^{1/2} \sim 0.2\,\mathrm{m\,s^{-1}}$ (for $l \sim 0.05$–$0.1\,\mathrm{m}$, $\delta T/T_0 \sim 0.1$)

$$u_T = \left(\frac{\delta T}{T_0}\right)^{1/2} u_*^{1/2} C_2(l, \nu, \kappa_T), \quad C_2 \approx gl Pr^{-1/4}(g\nu)^{-1/2}; \tag{20}$$

for large values of $u_* \gg u_2$

$$u_T = \left(\frac{\delta T}{T_0}\right)^{-1/2} u_*^{5/2} C_3(\nu, \kappa_T), \quad C_3 \approx (g\nu)^{-1/2} Pr^{-1/6}. \tag{21}$$

The dimensional factors C_1, C_2, C_3 in (Eqs. 19–21) are determined only by physical constants and the horizontal length scale l of velocity perturbations. Relations (Eqs. 19 and 20) for u_T regarded as a function of δT show that for small and moderate values of u_*, the exponent α in $u_T \sim (\delta T)^\alpha$ varies slightly in the range $1/2 < \alpha < 2/3$. However, for large u_*, the horizontal velocity amplitude at the thermal boundary layer height decreases with growing δT, $u_T \sim (\delta T)^{-1/2}$. The sign of α is changed for $u_* \approx 0.3\,\mathrm{m\,s^{-1}}$.

ACPD
11, 31231–31263, 2011

3.3 The mass concentrations dynamic

These dependencies are used to estimate the aerosol amount within the surface boundary layer in a Caspian desert. The basic external parameters include u_*, which is determined from measured profiles of the horizontal velocity, and the temperature difference δT in the viscous thermal boundary layer. The velocity and temperature are rather difficult to measure at the thermal boundary layer height δ_T, which is on the order of 1 cm. In fact, we can only determine the temperature difference δT between the sand surface and height 0.2 m and estimate u_* from measured profiles of the horizontal velocity. This value of δT is a good estimate of the temperature drop in a viscous thermal boundary layer, since the temperature variations above this layer are relatively weak.

As was mentioned in the Introduction, our basic assumption is that the difference between the mass concentrations at two levels – near the surface and above the thermal boundary layer ΔC – is proportional to the velocity amplitude u_T at the thermal boundary layer height δ_T:

$$\Delta C \sim u_\mathrm{T} - u_{T_\mathrm{cr}} . \tag{22}$$

The two quantities $\delta_\mathrm{T}, u_\mathrm{T}$ are determined from measured δT and u_* according to formulas (17–21). The proportionality of the velocity in Eq. (22) implies that, on the one hand, aerosol resuspension from the upper soil layer is enhanced with increasing u_T. On the other hand, the high horizontal velocity near the underlying surface impedes the settling of previously lifted aerosol particles.

Some substantiations of the formula (22) can be gained from a diffusion equation for a fine dispersed dust in an viscous-thermal layer of air immediately adjoining a surface of soil,

$$\frac{\partial C}{\partial t} + \frac{\partial w(z)C}{\partial z} = \kappa_\mathrm{c}\frac{\partial^2 C}{\partial z^2}, \quad z>0; \quad C = C_0, \quad z=0. \tag{23}$$

In this equation, for concentration C it is neglected by feeble variability across horizontal

ACPD
11, 31231–31263, 2011

Dust resuspension under weak wind conditions

O. G. Chkhetiani et al.

coordinates; κ_c is the kinematic diffusion of considered dust. Equation (23) guesses that the dust is fine dispersed. So, that gives the possibility to be restricted to approach with the written-out member of diffusion type. We suppose that the soil is a source of dust with concentration on surface C_0. Firstly, we consider the case of relative small friction velocity u_*. In these conditions $\delta_T < \delta_*$, so the second addend in the right part (Eq. 16) for u_T does not exceed the convective contribution $\frac{w_T l}{\delta_T}$. Then vertical velocity $w(z)$ in Eq. (23) can be approximated by linear function

$$w(z) \approx \frac{w_T}{\delta_T} \cdot z \sim \frac{u_T}{l} \cdot z \,. \tag{24}$$

From Eqs. (23) and (24) in the stationary conditions we obtain

$$\frac{\partial f_C}{\partial z} = 0, f_C = C \frac{u_T}{l} z - \kappa_c \frac{\partial C}{\partial z} \,. \tag{25}$$

Here, f_C is the dust flux from the surface. Equation (25) gives the solution

$$\begin{aligned} C(z) &= \left(C_0 - \frac{f_C}{\kappa_c} \int_0^z \exp\left(-\frac{u_T \zeta^2}{2 l \kappa_c} \right) d\zeta \right) \exp\left(-\frac{u_T z^2}{2 l \kappa_c} \right) \\ &\approx C_0 - z \frac{f_C}{\kappa_c} + \left(C_0 - z \frac{2 f_C}{3 \kappa_c} \right) \frac{u_T z^2}{2 l \kappa_c} \,. \end{aligned} \tag{26}$$

Here, due to the smallness of the height z, we consider only the first terms of the exponent decomposition, supposing that the diffusion coefficient κ_c is enough major so a thickness of a diffusion layer is more than a thickness of thermal δ_T and viscous δ_* layers. For fixed $z = z_0 \sim \delta_* > \delta_T$, we have a condition of turbulent mixing. Therefore, concentration $C(z_0)$ is a boundary for processes in this layer. For the difference ΔC between $C(z_0)$ and background $C(\infty)$ (for the measuring presented in the previous paragraph, $C(2.0)$ or $C(1.5)$), it is possible to express as

$$\Delta C = \gamma (u_T - u_{Tcr}), \tag{27}$$

ACPD
11, 31231–31263, 2011

$$\gamma = \left(C_0 - z\frac{2f_C}{3\kappa_c}\right)\frac{z_0^2}{2l\kappa_c}, \tag{28}$$

$$\gamma u_{T_{cr}} = C(\infty) - \left(C_0 - z\frac{f_C}{\kappa_c}\right). \tag{29}$$

This difference can be considered as an approximation of a difference of the measured concentrations of the previous paragraph.

In the case of great values of friction velocity u_* when $\delta_T > \delta_*$ so the viscous layer immediately adjoins soil, Eq. (23) can be considered in a thermal layer $\delta_* < z < \delta_T$ with $C = C_0$ on external boundary of a viscous layer, $z = z_* = \delta_*$. In the upper thermal part, we have $w(z) \approx u_*$ (see Eq. 16), so

$$f_C = u_* C - \kappa_c \frac{\partial C}{\partial z}.$$

As a result, at $z_0 = \delta_T$ we will obtain the formula similar to Eq. (26):

$$C(z_0) \approx C_0 - z_0\frac{f_C}{\kappa_c} + \left(C_0 - z_0\frac{f_C}{2\kappa_c}\right)\frac{u_T\delta_*}{\kappa_c}, \tag{30}$$

where for u_T approximation by the second addend of the right part (Eq. 16) was used. From here follows Eq. (27), where

$$\gamma = \left(C_0 - z_0\frac{f_C}{2\kappa_c}\right)\frac{\delta_*}{\kappa_c}, \quad \gamma u_{T_{cr}} = C(\infty) - \left(C_0 - z_0\frac{f_C}{\kappa_c}\right).$$

In view of Eq. (22) with $u_T \gg u_{T_{cr}}$, formulas (19, 20, 21) for u_T imply that, for small and moderate values of u_*, the exponent α in

$$\Delta C \sim (\delta T)^\alpha \tag{31}$$

ranges between 1/2 and 2/3. For large u_*, the aerosol mass concentration ΔC decreases like $(\delta T)^{-1/2}$ with increasing δT. This behavior of ΔC is shown in Figs. 4,

ACPD
11, 31231–31263, 2011

6, 7 with $\alpha = 0.58$ (Fig. 4a), $\alpha = 0.52$ (Fig. 4b), $\alpha = 0.33$ (Fig. 4c), $\alpha = 0.24$ (Fig. 4d), $\alpha = -0.5$ (Fig. 6a, 30 July 2007), $\alpha = -0.35$ (Fig. 6a, 31 July 2007), $\alpha = -0.35$ (Fig. 6c), $\alpha = 0.39$ (Fig. 7a), $\alpha = -0.21$, $\alpha = -0.17$ (Fig. 7b), $\alpha = 0.25$ (Fig. 7c), and $\alpha = -0.15$ (Fig. 7d).

3.4 The heat flux as the external parameter

In Obukhov (1971); Monin and Yaglom (1971); Lumley and Panofsky (1964), the basic parameter determining convection is the turbulent heat flux rather than δT. For comparison purposes, the formulas derived above can be rewritten in terms of a given heat flux f from the underlying surface. Simultaneously, the flow parameters in the thermal boundary layer can be estimated as functions of u_*, since f exhibits smaller variations than δT when the ground surface is heated to its maximum temperature. Specifically, f is determined only by insolation and the soil properties, while δT depends on f and the wind near the surface.

To proceed from the temperature difference to the heat flux, the temperature equation in Eq. (3) is integrated over the height z from 0 to δ_T, assuming that the basic temperature variations occur in the layer $0 < z < \delta_\mathrm{T}$ and, for $z \sim \delta_\mathrm{T}$, the lapse rate is much less than that at the surface $z = 0$. Then, after integrating, the term $\partial wT'/\partial z$ gives the estimate $w_\mathrm{T}\delta T$, while the term $\kappa_\mathrm{T}(\partial^2 T'/\partial z^2)$ leads to $-\kappa_\mathrm{T}\partial T'/\partial z|_{z=0} = f/\rho c_p$:

$$w_\mathrm{T}\delta T \approx \frac{f}{\rho c_p}\,, \tag{32}$$

where f is the heat flux from the surface $z = 0$.

Combined with (Eqs. 5, 6, 13–16), this relation yields the following estimates for δT and δ_T in terms of f and u_*:

$$\delta_\mathrm{T} \approx h\left(\frac{\delta T}{T_0}\right)^{-1}, \quad h = \left(\nu f/g\rho c_p T_0\right)^{1/2}, \tag{33}$$

ACPD
11, 31231–31263, 2011

Dust resuspension under weak wind conditions

O. G. Chkhetiani et al.

$$\frac{\delta T}{T_0} \approx \left(\frac{gh^3}{\nu\kappa_T}\right)^{1/2}\left(1-\frac{u_*^2}{gh}\right)^{1/2}, \tag{34}$$

$$\frac{\delta T}{T_0} \approx \frac{hu_*}{2\kappa_T}\left[\left(1+\frac{4gh}{Pru_*^2}\right)^{1/2}-1\right] \tag{35}$$

where the first estimate Eq. (34) is valid for $u_*^2/gh \leq Pr/(1+Pr)$, and second estimate Eq. (35) is valid for $u_*^2/gh \geq Pr/(1+Pr)$.

Here, h is the length scale Eq. (33) determined by the heat gain and viscosity.

In view of Eq. (33) and $u_* = 0$, the relation in Eq. (34) gives the well-known dependence $\delta T \sim f^{3/4}$ (see Golitsyn, 1980). It also follows from Eq. (35) that δT decreases with increasing u_* with the dependence for high friction velocities ($u_*^2 \gg gh$) as

$$\frac{\delta T}{T_0} \approx \frac{gh^2}{\nu}\frac{1}{u_*} = \frac{f}{u_* T_0 \rho c_p} = \frac{u_f}{u_*}, \tag{36}$$

where $u_f = f/\rho c_p T_0$ is the heat transfer rate introduced by Obukhov (1971). The thermal boundary layer thickness δ_T is then determined by the formula

$$\delta_T \approx u_* \frac{\nu}{gh} = h\frac{u_*}{u_f}.$$

Since the right-hand side of Eq. (36) does not involve the viscosity or thermal diffusivity, formula (36) gives (up to the von Karman constant) the well-known temperature scale for the atmospheric surface layer, the only quantity of the dimension of temperature that can be made up of u_*, $f/c_p\rho$. Note that h is small; for example, for the heat flux $f = 500\,\mathrm{W\,m^{-2}} = 5\times10^5\,\mathrm{g\ s^{-3}}$ (see the Sect. 1), $h \sim 10^{-4}$ m.

Decreasing δT with increasing u_* that follows from Eq. (35) and is seen from the measurements data (Fig. 8), by use of estimates Eqs. (17–19), Eq. (22) leads to the

ACPD
11, 31231–31263, 2011

decreasing the values of ΔC. Figure 9a–c shows ΔC measured at moderate values of u_*. In fact, this means that convective aerosol emission from the soil can be more effective in the absence of wind (low friction velocities, $u_* < 0.08$–$0.2\,\mathrm{m\,s^{-1}}$ in Fig. 9a–c) than in moderate wind (when $0.1\,\mathrm{m\,s^{-1}} < u_* < 0.2$–$0.3\,\mathrm{m\,s^{-1}}$, Fig. 9d). For the last values of u_*, the deviations ΔC are nearly constants that follow from the estimate Eq. (36) for δT and Eq. (20) for u_T.

As the end of this section, it should be noted that, according to Eqs. (19–21), the linearity in Eq. (22) with respect to u_T does not mean linearity with respect to u_*. Moreover, for large u_* (see Eq. 21), the mass concentration ΔC is proportional to $u_*^{5/2}$ for fixed δT and $\Delta C \sim u_*^3$ if f is given: $(\frac{\delta T}{T_0})^{-1/2} \sim u_*^{1/2}$ (see Eq. 36). The fine dispersed particles flux from the soil surface $z = 0$ is equal to $f_C = -\kappa_\mathrm{c} \frac{dC}{dz}|_{z=0}$ (see Eq. 25). As an estimate, we can accept $f_C \sim \kappa_\mathrm{c} \frac{|\Delta C|}{\delta z}$, where δz is the difference of the measurements levels. So, for given heat flux f we obtain Bagnold's dependence u_*^3. This circumstance can serve as an additional argument for assumption Eq. (22), apart from its obvious simplicity. For fine dispersed fraction, the dependence $\sim u_*^3$ was obtained also in the laboratory measurements presented in Loosmore and Hunt (2000).

4 Conclusions

The underlying assumption in this work is that fine aerosol resuspension from the soil is proportional to the horizontal air velocity u_T at the height of the thermal boundary layer. In addition to the obvious simplicity of this hypothesis, another supporting argument is that it implies Bagnold's law u_*^3 for relatively high friction velocities: an increase in u_T leads to resuspension of not only fine aerosol but also coarse soil particles that satisfy this law. However, it should be noted that the last empirical law holds when u_* is higher than the threshold value ~ 0.4–$0.5\,\mathrm{m\,s^{-1}}$. The thermal factors then become not very significant, and sand and aerosol are carried away by strong turbulent velocity

Discussion Paper | Discussion Paper | Discussion Paper | Discussion Paper |

ACPD
11, 31231–31263, 2011

Dust resuspension under weak wind conditions

O. G. Chkhetiani et al.

fluctuations, ensuring the rolling and saltation of numerous particles at the ground surface. In this work, primary attention was given to the thermal factors at relatively low friction velocities associated with the mean wind shear.

Measurements show that the fine aerosol in the chosen region constitutes a considerable fraction of the entire air aerosol in the atmospheric surface layer (in terms of both the number of particles and their mass). Also, the difference between the aerosol concentrations at two near-ground levels depends both on the temperature difference δT in the viscous thermal sublayer and on u_* in the overlying turbulent mixing layer. The use of concentration differences ΔC yields clearer dependencies than the use of the concentrations $C(z)$ at near-ground levels, since the latter can be more variable and depends on the conditions preceding the measurements. This can be seen in Fig. 5.

For low and moderate friction velocity u_*, formulas (19 and 20) and Figs. 4 and 7a,c show that, as δT grows, u_T increases with positive exponent α (ranging from 1/2 to 2/3 in the model of convection). For large u_*, as δT grows, u_T falls off with negative exponent α (Figs. 6 and 7b,d).

The estimates of the model (Eqs. 17, 19–21, 34–35) show that the convective resuspension of fine aerosols in no wind or light wind can be more effective than in moderate wind. This is demonstrated in Figs. 9a–c for several days of measurements.

Of course, for stronger winds ($u_* > 0.3$–$0.4\,\mathrm{m\,s^{-1}}$, Fig. 9d), the dependence on u_* changes. However, as was mentioned at the beginning of the Introduction, for this case the basic mechanism for aerosol emission from the soil is the rolling and saltation of large particles sticking out of the viscous boundary layer δ_* under the action of wind.

Thus, as expected, the dynamics of air and aerosol transport in adjacent layers with different physical and hydrodynamic properties represent a complicated problem requiring substantially different approaches to its solution.

Acknowledgements. This work was initiated 15 years ago by I. G. Granberg and V. M. Ponomarev. The authors are grateful A. A. Khapaev, V. K. Bandin, I. A. Bouchnev, B. A. Khartskhaev, S. A. Kosyan, V. A. Lebedev, F. A. Pogarskii, I. A. Repina and B. V. Zoudin for the help in the field measurements. The authors are grateful to G. S. Golitsyn for his interest in this work

ACPD

11, 31231–31263, 2011

and helpful remarks. This work was supported by the Russian Foundation for Basic Research (project nos. 10-05-01110).

References

Climate Change 2007: The Physical Science Basis, Cambridge Univ. Press, New York, 940 pp., 2007. 31232

Golitsyn, G. S., Granberg, I. G., Andronova, A. V., Ponomarev, V. M., Zilitinkevich, S. S., Smirnov, V. V., and Yablokov, M. Y.: Investigation of boundary layer fine structure in arid regions, Water Air Soil Pollut. Focus, 3, 245–257, 2003. 31232, 31234

Bagnold, R. A.: The Physics of Blown Sand and Desert Dunes, Methuen, New York, 265 pp., 1941. 31235

Barenblatt, G. I. and Golitsyn, G. S.: Local structure of mature dust storms, J. Atmos. Sci., 31, 1917–1933, 1974. 31232

Batchelor, G. K.: An Introduction to Fluid Dynamics, Cambridge Univ. Press, Cambridge, 615 pp., 1967.

Foken, T. H.: The molecular temperature boundary layer of the atmosphere over various surfaces, Arch. Met. Geoph. Biokl. A, 27, 59–67, 1978. 31233

Foken, T. H.: Micrometeorology, Springer-Verlag Berlin Heidelberg, 306 pp., 2008. 31233, 31241

Gillette, D. A. and Sinclair, P. C.: Estimation of suspension of alkaline material by dust devils in the United States, Atmos. Environ. A, 24, 1135–1142, 1990. 31234

Gillette, D. A., Fryear, D. W., Gill, T. E., Ley, T., Cahill, T. A., and Gearhart, E. A.: Relation of vertical flux of particles smaller than 10 µm to total aeolian horizontal mass flux at Owens Lake, J. Geophys. Res., 102, 2609–26015, 1993. 31234

Gillette, D. A., Lawson, Jr., R. E., and Thompson, R. S.: A “test of concept” comparison of aerodynamic and mechanical resuspension mechanizms for particles deposited on field rye grass. Part 1 – Relative particle flux rates, Atmos. Environ., 38, 4789–4797, 2004. 31234

Gledzer, E. B., Granberg, I. G. and Chkhetiani, O. G.: Air dynamics near the soil surface and convective emission of aerosol izvestiya, Atmos. Ocean. Phys., 46, 29–40, 2010. 31241, 31245

Golitsyn, G. S.: Simple theoretical and experimental study of convection with some geophysical applications and analogies, J. Fluid Mech., 95, 567–608, 1980. 31234, 31241, 31250
Greeley, R. and Iversen, J. D.: Wind as a geological process on Earth, Mars, Venus and Titan, Cambridge University Press, New York, 333 pp., 1985. 31234
Junge, C.: Air chemistry and radioactivity, Academic Press, New York, 382 pp., 1963. 31237
Kok, J. F. and Renno, N. O.: A comprehensive numerical model of steady state saltation (COMSALT), J. Geophys. Res., 114, D17204, doi:10.1029/2009JD011702, 2009. 31235
Landau, L. D. and Lifshitz, E. M.: Fluid Mechanics, Pergamon, Oxford, 539 pp., 1987.
Larsen, S. E., Jorgensen, H. E., Landberg, L., an Tillman, J. E.: Aspects of the atmospheric surface layers on Mars and Earth, Bound.-Lay. Meteorol., 105, 451–470, 2002. 31234
Lumley, J. L. and Panofsky, H. A.: The Structure of Atmospheric Turbulence, Interscience Publishers, New York, 239 pp., 1964. 31241, 31249
Loosmore, G. A. and Hunt, J. R.: Dust resuspension without saltation, J. Geophys. Res, 105, 20663–20671, 2000. 31234, 31251
Monin, A. S. and Yaglom, A. M.: Statistical Fluid Mechanics, vol. 1, MIT Press, Cambridge, London, 769 pp., 1971. 31233, 31249
Obukhov, A. M.: Turbulence in an atmosphere with a non-uniform temperature, Bound.-Lay. Meteorol., 2, 7–29, 1971. 31241, 31249, 31250
Shao, Y.: Physics and modelling of wind erosion, Kluwer Academic, Boston, 452 pp., 2000. 31235, 31236
Yablokov, M. Y. and Andronova, A. V.: A model of takeoff processes of desert sand aerosols in windless conditions, J. Aerosol. Sci. 28(Suppl 1), 563–564, 1997. 31233
Zhou, Y., Guo, X., and Zheng, X. J.: Experimental measurements of wind-sand flux and sand transport for naturally mixed sands, Phys. Rev. E, 66, 021305(1–9), 2002. 31235
Wang, H. C.: Effect of inceptive motion on particle detachment from surfaces, Aerosol. Sci. Technol., 13, 386–393, 1990.

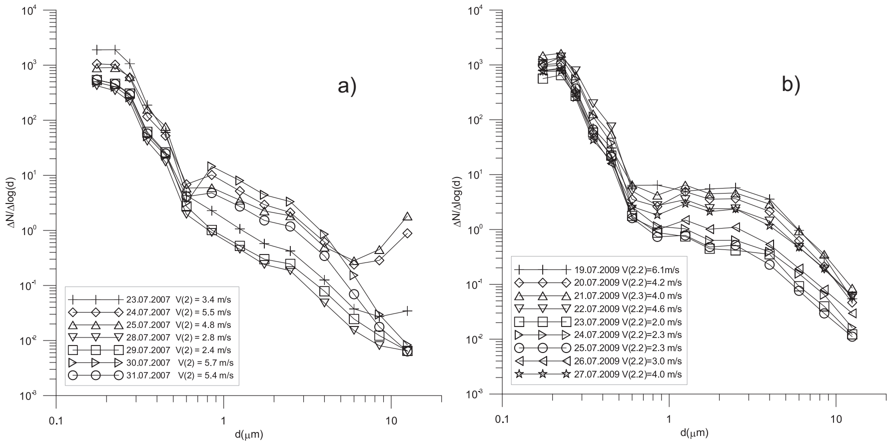

Fig. 1. Daytime-averaged at 2 m distributions **(a)** for 2007, **(b)** for 2009 of aerosol particles account; inserts: the daytime-averaged horizontal velocity at 2 m (for 2007) and 2.2 m (for 2009).

ACPD
11, 31231–31263, 2011

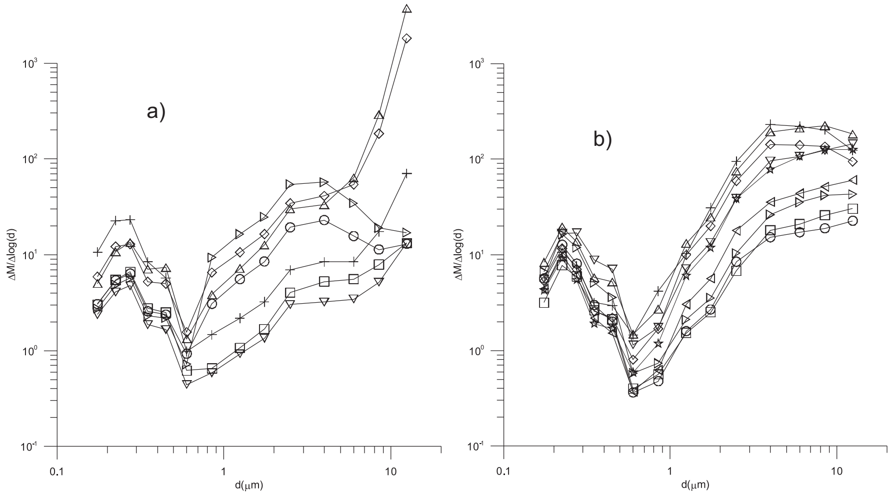

Fig. 2. Daytime-averaged at 2 m distributions **(a)** for 2007, **(b)** for 2009 of aerosol particles mass concentrations with the particles size; inserts: the daytime-averaged horizontal velocity at 2 m (for 2007) and 2.2 m (for 2009).

ACPD
11, 31231–31263, 2011

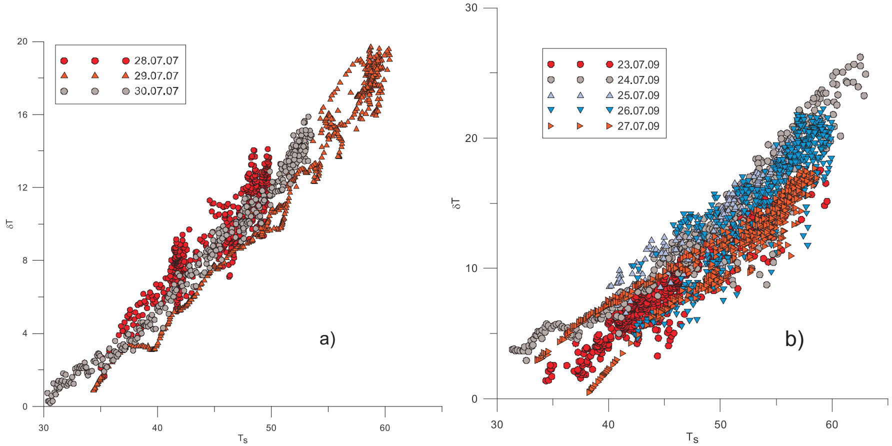

Fig. 3. The temperature differences δT between the ground surface temperature T_s (°C) and temperature at 0.2 m: **(a)** data of 28–30 July 2007, **(b)** data of 23–27 July 2009.

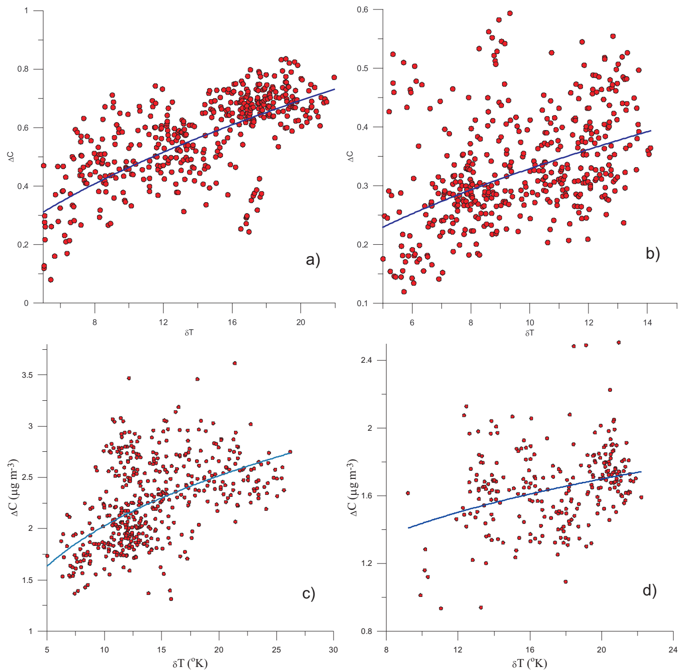

Fig. 4. Deviations of the aerosol mass concentrations at 0.5 m from the 2-m values (for 2007) and 1.5-m (for 2009) ($\mu g\,m^{-3}$) for particles 0.15–0.5 µm in size (for 2007) and 0.15–1.0 µm (for 2009) as a function of the temperature difference δT between the ground surface and 0.2 m. **(a)** data of 29 July 2007; the 2-m daytime averaged wind speed is 2.4 $m\,s^{-1}$, and $u_* < 0.2\,m\,s^{-1}$; the smooth line corresponds to the approximation $\Delta C \sim \delta T^{0.58}$; **(b)** data of 28 July 2007; the 2-m wind speed is 2.8 $m\,s^{-1}$, and $u_* < 0.3\,m\,s^{-1}$; the smooth line – $\Delta C \sim \delta T^{0.52}$; **(c)** data of 24 July 2009; the 2.2-m wind speed is 2.0 $m\,s^{-1}$ (in the morning), and $u_* < 0.2\,m\,s^{-1}$; the smooth line – $\Delta C \sim \delta T^{0.33}$; **(d)** data of 26 July 2009; the 2.2-m wind speed is 3.0 $m\,s^{-1}$, and $u_* < 0.3\,m\,s^{-1}$; the smooth line – $\Delta C \sim \delta T^{0.24}$.

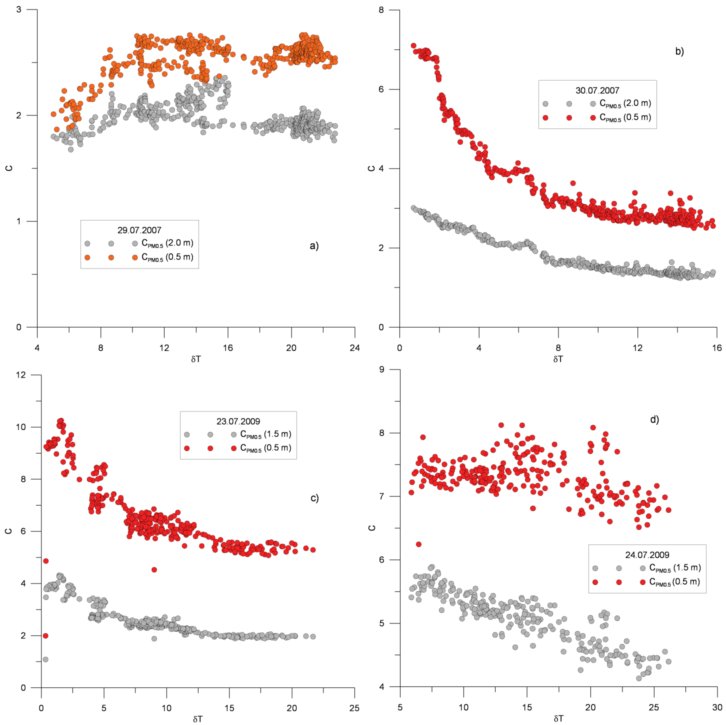

Fig. 5. Mass concentration at 0.5 m $C(0.5)$ and 2 m $C(2.0)$ – for **(a,b)**, 1.5 m $C(1.5)$ for **(c,d)** ($\mu g\,m^{-3}$) for particles 0.15–0.5 µm in size as a function of the temperature difference δT between the ground surface and 0.2 m: **(a)** – for 29 July 2007, **(b)** – for 30 July 2007, **(c)** – for 23 July 2009, **(d)** – for 24 July 2009.

ACPD
11, 31231–31263, 2011

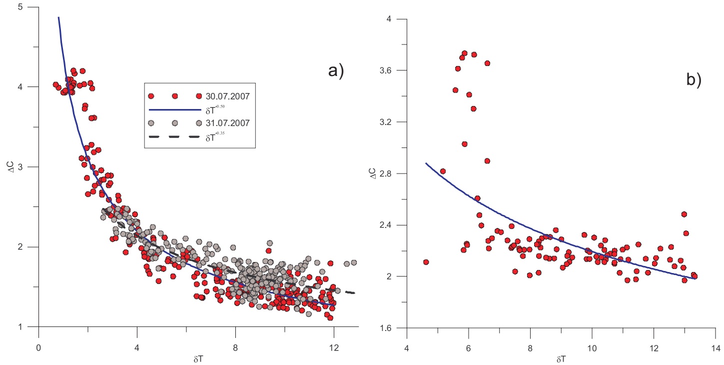

Fig. 6. Deviations of the aerosol mass concentrations at 0.5 m from the 2-m values (for 2007) and 1.5-m (for 2009) ($\mu g\,m^{-3}$) for particles 0.15–0.5 µm in size as a function of the temperature difference δT between the ground surface and 0.2 m; **(a)** the 2-m daytime averaged wind speed is 5.7 $m\,s^{-1}$ for 30 July 2007, and 5.4 $m\,s^{-1}$ for 31 July 2007, solid line depicts the approximation $\Delta C \sim \delta T^{-0.5}$ for 30 July 2007 and dashed line – $\Delta C \sim \delta T^{-0.35}$ for 31 July 2007; **(b)** the 2.2-m wind speed is 3.0 $m\,s^{-1}$ for 26 July 2009, solid line – $\Delta C \sim \delta T^{-0.35}$.

ACPD
11, 31231–31263, 2011

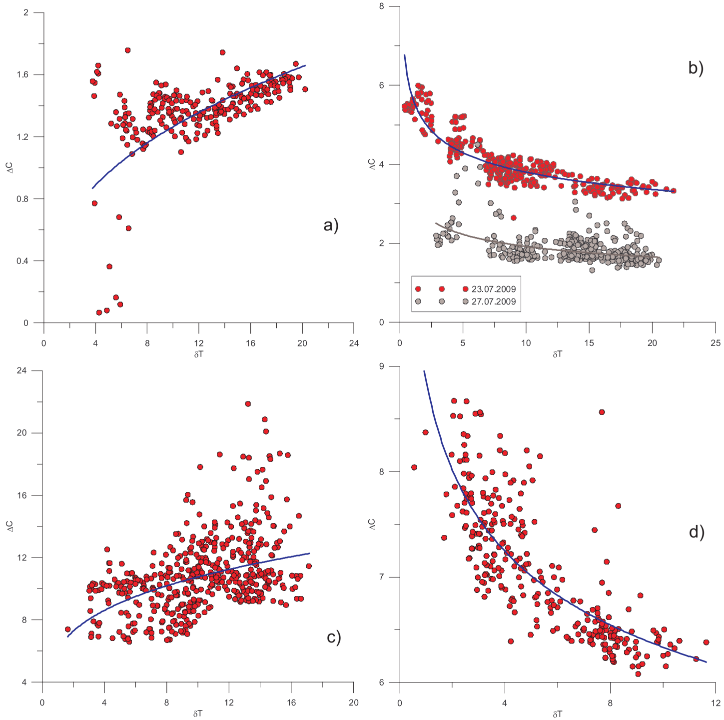

Fig. 7. Deviations of the aerosol mass concentrations at 0.5 m from 1.5-m (for 2009) (µg m^{-3}) for particles 0.15–0.5 µm as a function of the temperature difference δT between the ground surface and 0.2 m; **(a)** for 27 July 2009, solid line – $\Delta C \sim \delta T^{0.39}$, **(b)** for 27 July 2009, solid line – $\Delta C \sim \delta T^{-0.21}$, for 23 July 2009, solid line – $\Delta C \sim \delta T^{-0.17}$, **(c)** for 27 July 2010, solid line – $\Delta C \sim \delta T^{0.25}$, **(d)** for 19 July 2010, solid line – $\Delta C \sim \delta T^{-0.15}$.

ACPD
11, 31231–31263, 2011

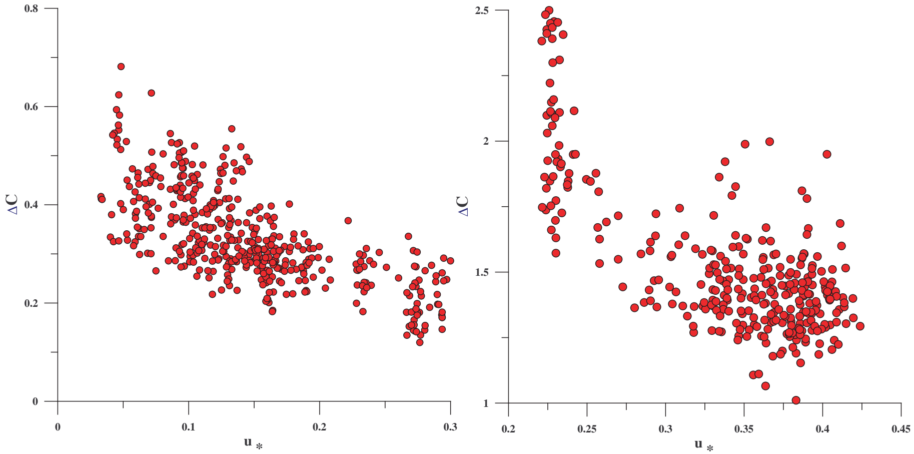

Fig. 8. Temperature drop δT across the thermal boundary layer as a function of u_* **(a)** for 28 July 2007, **(b)** for 27 July 2009.

ACPD
11, 31231–31263, 2011

Dust resuspension under weak wind conditions

O. G. Chkhetiani et al.

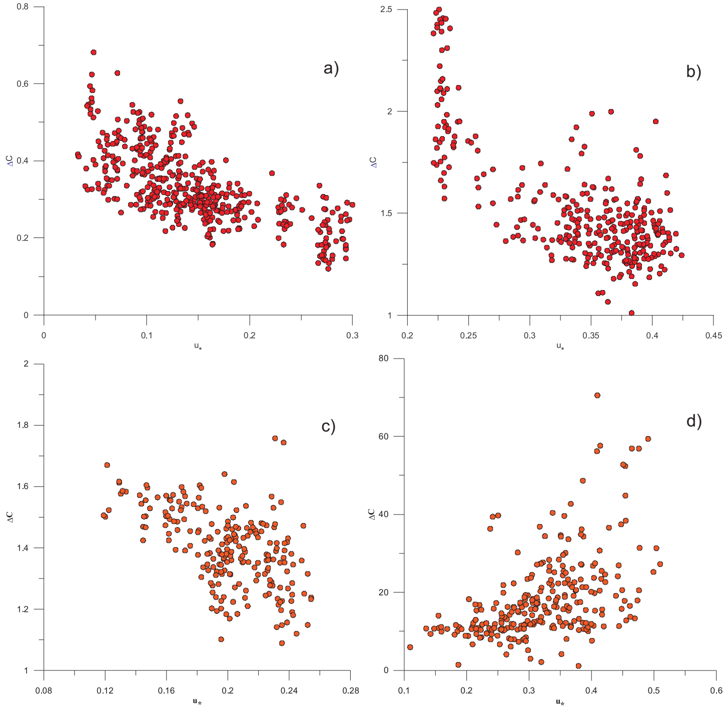

Fig. 9. Deviation of the 0.5-m aerosol mass concentration from the background value at 2 m (2007) or 1.5 (2009)(µg m^{-3}) for particles 0.15–0.5 µm in size as a function of the friction velocity u_*: **(a)** – 28 July 2007, **(b)** – 30 July 2007, **(c)** – 27 July 2009, **(d)** – 20 July 2010.